Reconstruction of 3-D VMEC equilibria with helical cores in DIII-D

A. Wingen[1], R.S. Wilcox[1], M.R Cianciosa[1], S.K. Seal[1], E.A. Unterberg[1],
S.P. Hirshman[1], P. Piovesan[2] and F. Turco[3]

[1] *Oak Ridge National Laboratory, Oak Ridge, Tennessee, USA*

[2] *Consorzio RFX, Padua, Italy*

[3] *Columbia University, New York, New York, USA*

High performance hybrid discharges [1] operate at conditions that are favorable for forming helical cores. In recent experiments at ASDEX and DIII-D, helical cores have been experimentally verified in such hybrid discharges [2]. In the following, we focus on the DIII-D experiment and show for the first time a reconstructed 3D helical core equilibrium in a tokamak. The reconstructed equilibrium can be used to numerically study the properties of an experimentally observed helical core. The latter is a 1/1 saturated internal kink [3], excited by 3D perturbation fields and driven primarily by the pressure gradient near q = 1, for various shapes of the q-profile with q_{min} close to unity. It is bifurcated from an axisymmetric state by 3D fields and flattens the q-profile in the core, with a potential to stabilize sawteeth.

The DIII-D discharge 164661 operates at $\beta = 2.56\%$ keeping beta, density, input power and other global plasma parameters constant after the hybrid discharge is established ($t >$ 1.5 s). Electron cyclotron current drive (ECCD) is applied during the discharge to suppress a 3/2 tearing mode, which is typical for hybrid operation. An $n = 1$ resonant magnetic perturbation (RMP) is applied at 3 s into the discharge, causing some density pump-out while beta is maintained. The hybrid discharge remains stable between about 3.5 s and 4.5 s with only very little 4/3 tearing mode activity. The RMP rotates at 20 Hz and thereby rotates any induced 3D structures past the available diagnostics. In particular, it was found in simulations that the helical core phase locks to an externally applied RMP field. Figure 1 shows a time trace of local soft-X-ray (SXR) emission along the major radius R at $Z = 0$. The SXR emission is obtained by a set of intersecting arrays that cover the entire volume. Tomographic inversion is used to calculate the local emission from the line-integrated

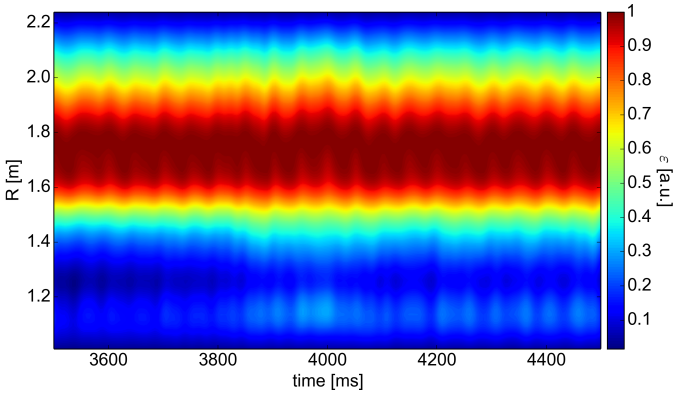

Figure 1: *Time evolution of the local soft X-ray emission along the major radius at Z = 0 in shot 164661.*

measurement. The SXR emission shows a typical "snake", which is produced by the 1/1 helical core rotating by the diagnostic with the applied RMP rotation frequency.

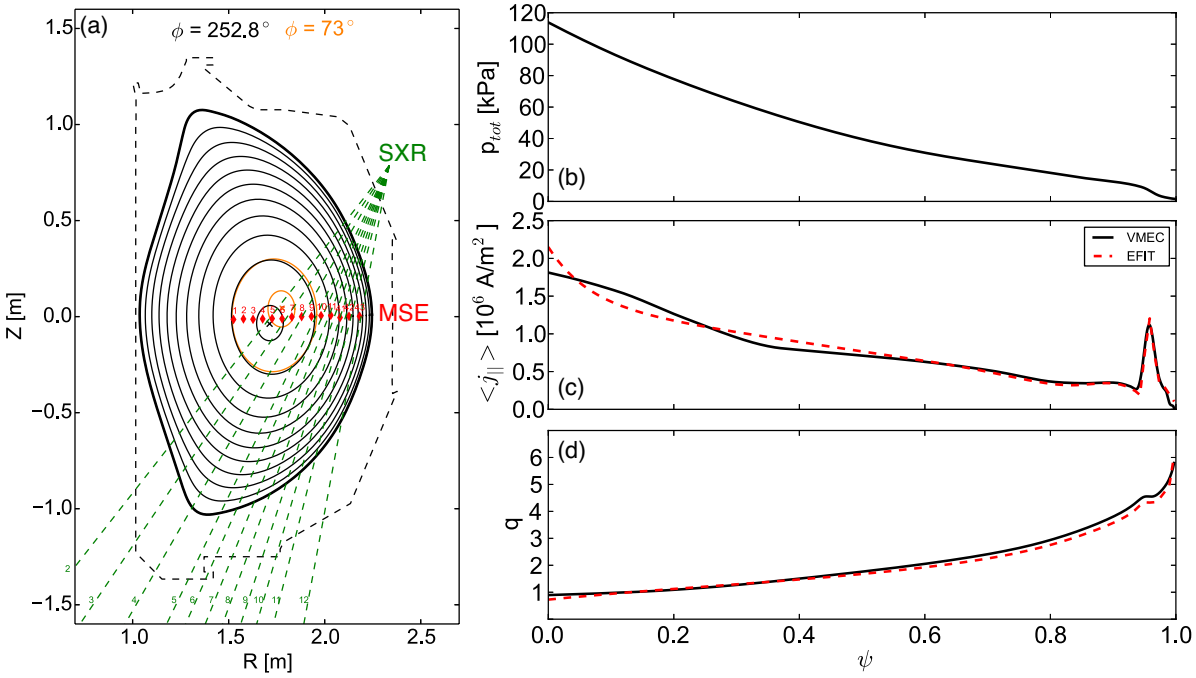

Figure 2: *Reconstructed VMEC equilibrium of shot 164661 at 4300 ms, schematically showing the helical core. (a) poloidal cross section overlayed for two toroidal angles, (b) pressure profile, (c) current density profile, the red dashed line shows the 2D EFIT result, (d) q-profile.*

For the reconstruction, a staged approach is used, starting out with an axisymmetric kinetic EFIT [4] reconstruction. Keeping the pressure profile fixed (as a function of poloidal flux) from EFIT, we take the axisymmetric boundary and perturb it by the applied RMP field using a free boundary VMEC simulation [5, 6]. This provides the initial equilibrium to the 3D reconstruction code V3FIT [7]. By identifying four time slices within a period of the RMP rotation with virtual diagnostics at 4 toroidal locations, the 3D information available to V3FIT is greatly increased. Using SXR and MSE data, an equilibrium is reconstructed that fits the measured data set as best as possible. Figure 2 shows the cross section and all relevant profiles, compared to the original axisymmetric EFIT. The equilibrium has a 3.7 cm helical displacement in the core. This is the first reconstruction of a helical core equilibrium in a tokamak. Measurement uncertainty propagation confirms that the uncertainty of the helical axis position is much smaller than the axis displacement.

VMEC simulations confirm that the helical core is a bifurcation of an axisymmetric state. Both can exist for the same plasma parameters, while the helical core state is excited by any kind of 3D seed perturbation, either a numerical "kick" to the axis or an RMP-induced helical ripple in the edge.

The comparison between these two states is shown in Fig 3. Here all plasma parameters are kept fixed, except for the total plasma current. Ramping up the current shifts the q-profile down without changing its shape, so q_{min} is lowered. In the axisymmetric state without any 3D perturbation, the relation between q_{min} and the current is linear, while in the helical state, the q-profile gets significantly flattened around $q = 1$. Especially in axisymmetric cases with $q_{min} < 1$, q is raised towards unity, with a potential to stabilize sawteeth. Fig. 2(d) confirms that with a helical core q increases for $\psi < 0.1$ compared to an axisymmetric (EFIT) state.

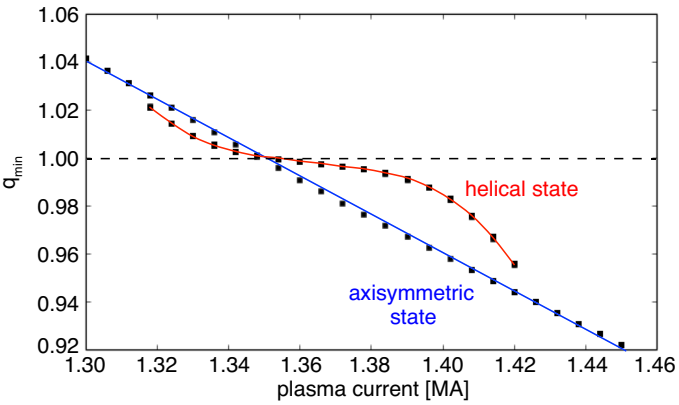

Figure 3: *Dependence of minimum of q-profile on total plasma current. Comparison between the axisymmetric and helical states.*

The helical core is driven primarily by the pressure gradient near the $q = 1$ surface. This is shown in Fig. 4, which shows the amplitude of the helical core $\delta_H = \sqrt{R^2_{n=1} + Z^2_{n=1}}/a$, with minor radius a and $n = 1$ helical component of the magnetic axis location (R, Z), for three different scalings of the pressure profile. For the black curve, the entire p-profile is scaled linearly, which raises β but also ∇p. The reconstructed helical core is at about 5% of the minor radius, but grows fast when β is increased. The blue line scales only the pressure in the core, scaling ∇p much more than β, while the red line scales only β, keeping ∇p fixed at $q = 1$. This shows that ∇p is the dominant driver for the helical core and confirms that the helical core is a saturated internal kink instability.

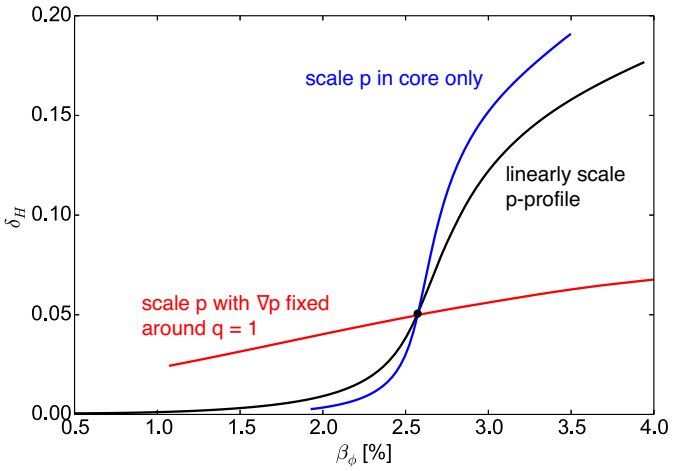

Figure 4: *Scaling of helical core amplitude with plasma β at different pressure gradient scalings. (black) linear scaling of p-profile, (blue) scaling of p in core only, (red) keep ∇p fixed at $q = 1$. The marker shows the reconstructed equilibrium condition.*

Changing the shape of the q-profile is another way to affect the helical core amplitude at a given pressure profile. Here we take the reconstructed current density profile in Fig. 2(c) and

change the location of a major amount of the plasma core current density in terms of a Gaussian peak. The total plasma current is thereby kept fixed. By moving the peak along the x-axis (ψ) to the left, the current density becomes more peaked in the core, while it becomes hollow if the peak is moved to the right. The latter eventually results in a reversed shear q-profile.

Figure 5 shows the dependence of the helical core amplitude δ_H on the Gaussian peak location and q_{min}. The latter is again scaled by scaling the total plasma current. The white circle marks the configuration of the reconstructed equilibrium. This shows that by moving more current off-axis, i.e. broadening the current density profile, the helical core grows significantly, even before the onset of a reversed shear q-profile. The largest helical cores are found for a reversed shear q-profile with $q_{min} = 1$.

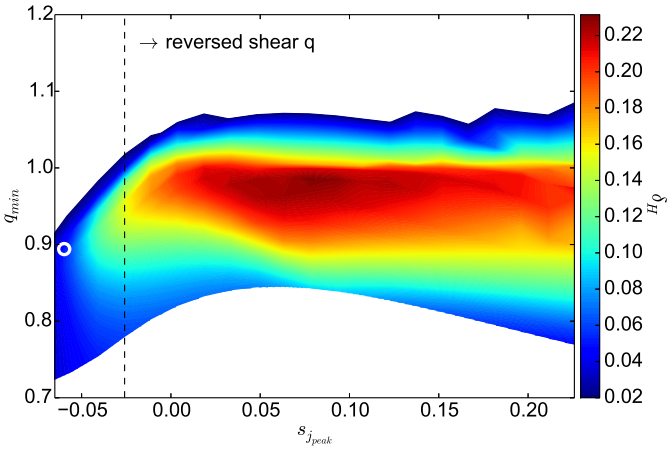

Figure 5: *Scaling of helical core amplitude with current density profile shape and minimum of q-profile.* $s_{j_{peak}}$ *marks the position of a Gaussian peak moving along the current density profile at constant total current. The circle marks the reconstructed equilibrium case.*

Both, increasing the core pressure gradient as well as increasing off-axis current density allows significant increases in the helical core amplitude. Further experiments could allow for a verification of the presented scalings and enable prediction and extrapolation of helical core amplitudes in hybrid discharges for today's and future machines like ITER.

This work is supported by DE-AC05-00OR227251, DE-FG02-04ER547612, DE-FC02-04ER546983 and DE-AC02-09CH114663 and used resources of the Oak Ridge Leadership Computing Facility.

References

[1] T. C. Luce *et al.*, Nuclear Fusion **43**, 321 (2003).

[2] P. Piovesan *et al.*, Impact of ideal MHD stability limits on high-beta hybrid operation, *here at this 43. EPS Conference*, I3.109.

[3] W. A. Cooper, J. P. Graves, and O. Sauter, Nuclear Fusion **51**, 072002 (2011).

[4] L. L. Lao, H. S. John, R. D. Stambaugh, A. G. Kellman, and W. Pfeiffer, Nuclear Fusion **25**, 1611 (1985).

[5] S. P. Hirshman, and J. C. Whitson Physics of Fluids **26**, 3553 (1983).

[6] A. Wingen *et al.*, Plasma Phys. Control. Fusion **57**, 104006 (2015).

[7] J. D. Hanson *et al.*, Nuclear Fusion **49**, 075031 (2009).